JPP Journal of Pharmacy and Pharmacology

JPP 2007, 59: 161–170

Received February 3, 2006
Accepted July 24, 2006
DOI 10.1211/jpp.59.2.0003
ISSN 0022-3573

Determination of amorphous content in the pharmaceutical process environment

Marja Savolainen, Kirsi Jouppila, Outi Pajamo, Leena Christiansen, Clare Strachan, Milja Karjalainen and Jukka Rantanen

Abstract

The amorphous state has different chemical and physical properties compared with a crystalline one. Amorphous regions in an otherwise crystalline material can affect the bioavailability and the processability. On the other hand, crystalline material can function as nuclei and decrease the stability of an amorphous system. The aim of this study was to determine amorphous content in a pharmaceutical process environment using near infrared (NIR) and Raman spectroscopic techniques together with multivariate modelling tools. Milling was used as a model system for process-induced amorphization of a crystalline starting material, α-lactose monohydrate. In addition, the crystallization of amorphous material was studied by storing amorphous material, either amorphous lactose or trehalose, at high relative humidity conditions. The results show that both of the spectroscopic techniques combined with multivariate methods could be applied for quantitation. Preprocessing, as well as the sampling area, was found to affect the performance of the models. Standard normal variate (SNV) transformation was the best preprocessing approach and increasing the sampling area was found to improve the models. The root mean square error of prediction (RMSEP) for quantitation of amorphous lactose using NIR spectroscopy was 2.7%, when a measuring setup with a larger sampling area was used. When the sampling area was smaller, the RMSEPs for lactose and trehalose were 4.3% and 4.2%, respectively. For Raman spectroscopy, the RMSEPs were 2.3% and 2.5% for lactose and trehalose, respectively. However, for the optimal performance of a multivariate model, all the physical forms present, as well as the process environment itself, have to be taken into consideration.

Division of Pharmaceutical Technology, Faculty of Pharmacy, P.O. Box 56, FI-00014 University of Helsinki, Helsinki, Finland

Marja Savolainen, Outi Pajamo, Leena Christiansen, Clare Strachan, Milja Karjalainen

Department of Food Technology, Faculty of Forestry and Agriculture, P.O. Box 66, FI-00014 University of Helsinki, Helsinki, Finland

Kirsi Jouppila

Drug Discovery and Development Technology Center (DDTC), Faculty of Pharmacy, P.O. Box 56, FI-00014 University of Helsinki, Helsinki, Finland

Clare Strachan, Jukka Rantanen

The Danish University of Pharmaceutical Sciences, Department of Pharmaceutics and Analytical Chemistry, Universitetsparken 2, 2100 Copenhagen, Denmark

Jukka Rantanen

Correspondence: J. Rantanen, The Danish University of Pharmaceutical Sciences, Department of Pharmaceutics and Analytical Chemistry, Universitetsparken 2, 2100 Copenhagen, Denmark. E-mail: jtr@dfuni.dk

Introduction

The solid state of material affects its physical, chemical and mechanical properties, such as solubility, melting point, stability, compressibility and flow properties (Grant 1999). Traditionally the crystalline state is the desired one, principally due to better stability. However, the amorphous state has some advantages compared with the crystalline state, such as higher solubility and dissolution rate. The disadvantage is that the amorphous state is a high-energy state and the material, thus, tends to crystallize during processing or storage at high temperature or relative humidity. Amorphous or partly amorphous materials are created intentionally by spray drying, freeze drying, quench cooling or grinding. However, they are often also created unintentionally during different unit operations, such as compression, micronization, dehydration or granulation (Vippagunta et al 2001). Even small quantities of amorphous material can affect the processability of otherwise crystalline material (e.g. due to increased hygroscopicity). On the other hand, if the amorphous state is the targeted solid state, small amounts of crystalline material can function as nuclei and lead to faster crystallization of the amorphous material. Therefore, a need exists in different fields of industry, such as the pharmaceutical or food industry, to be able to determine the amount of amorphous material created during processing. Current regulatory thinking also encourages towards the implementation of process analytical technologies (PAT). For example, the Food and Drug Administration (FDA) has introduced a PAT guidance, where the aim is to change from end-product control to process analytical techniques (FDA 2004). The aim is to increase science-based process and product understanding.

Previous studies have shown that both Raman and near infrared (NIR) spectroscopies can be used to determine the crystallinity of materials (Buckton et al 1998; Taylor & Zografi 1998; Gombás et al 2004; Niemelä et al 2004; Nørgaard et al 2005). Traditionally the quantitation is based on a univariate or bivariate model, such as peak height or area. Often the specific peaks used for the quantitation are overlapping or the differences in the crystalline and amorphous spectra are vague, which makes the quantitation more difficult. These problems are overcome in multivariate approaches, such as a partial least squares (PLS) model, where whole spectra can be used to build up the model. Spectroscopic techniques have been used to monitor different processes such as crystallization, blending, and granulation in real time. However, to the best of our knowledge they have not been previously used in a process environment to follow changes in the amorphous content in real time.

The aim of this study was to create a quantitation method to determine the amorphous content of materials in a process environment. Two spectroscopic techniques (NIR and Raman) were used in real-time mode. The change in amorphousness was studied in two different model process environments: grinding of crystalline material and crystallizing the amorphous material during storage at high relative humidity.

Materials and Methods

Materials and related unit operations

Preparation of amorphous materials

α-Lactose monohydrate (Pharmatose 200M; DMV International, Veghel, The Netherlands) and trehalose dihydrate (SigmaAaldrich Chemie Gmbh, Steinheim, Germany) were used as model substances. Amorphous lactose and trehalose were prepared by spray drying (Büchi Mini Spray Dryer B-191; Büchi Labortechnik AG, Flawil, Switzerland) 15% (w/w) solutions from lactose monohydrate and trehalose dihydrate, respectively. Spray-dried particles were dried at 40°C for 24 h to remove the excess moisture and stored in vacuum desiccators at relative humidity (r.h.) of 0% (over P_2O_5) at room temperature for a week before preparation of the binary mixtures.

Binary mixtures

Binary mixtures of amorphous lactose and α-lactose monohydrate, as well as amorphous trehalose with trehalose dihydrate were mixed in different weight/molar ratios. The content of amorphous component varied between 0 and 100% (w/w). In total, 19 different weight ratios were prepared from lactose (0.0, 1.0, 3.0, 5.0, 10.0, 20.0, 30.0, 40.0, 47.0, 50.0, 53.0, 60.0, 70.0, 80.0, 90.0, 95.0, 93.0, 99.0 and 100.0% (w/w) corresponding to 0.0, 1.1, 3.2, 6.3, 10.5, 20.8, 31.1, 41.2, 48.3, 51.3, 54.3, 61.2, 71.1, 80.8, 90.5, 97.1, 99.0 and 100.0 mol%) and 11 different weight ratios from trehalose (0, 10, 20, 30, 40, 50, 60, 70, 80, 90 and 100% (w/w) corresponding to 0.0, 10.9, 21.6, 32.1, 42.4, 52.5, 62.4, 72.1, 81.6, 90.9 and 100.0 mol%). Each composition was done in triplicate. In this study, a sample that caused no distinct reflections in the X-ray powder diffraction pattern was considered completely amorphous. After preparation the samples were stored in vacuum desiccators at 0% r.h. (silica gel). α-Lactose monohydrate and trehalose dihydrate contained 5.0% and 9.5% of water, respectively. Thus, they only contained the hydrate water. The water content in the amorphous material was insignificant.

Amorphization of crystalline material (ball milling)

Crystalline α-lactose monohydrate was ground in a ball mill (Pulverisette 6, Fritsch GmbH, Idar-Oberstein, Germany). The rotation speed was 400 rev min^{-1} and the ball-to-mass ratio was 10:1. Raman and NIR spectra of the ground samples were determined directly from the grinding bowl after 5, 10, 15, 30, 45, 60, 75, 90, 105, 120, 150 and 180 min grinding. For comparison, X-ray powder diffraction (XRPD) patterns were determined from the same time points. Raman and NIR spectra, as well as XRPD patterns, were determined using the methods described in the Physical characterization of materials section, below. A Savitzky-Golay smoothing algorithm was performed on the Raman data. For the NIR, the lamp setup was used. Raman and NIR spectra were measured in triplicate.

Crystallization of amorphous material (at high relative humidity)

Amorphous lactose and trehalose were stored in a humidity chamber at 85% r.h. The crystallization of amorphous lactose was followed in-line with NIR and Raman spectroscopy using the method described in the Physical characterization of materials section. The sample size in both the NIR and Raman experiments was 1.0 g. In the NIR experiments, the sample was stored in a glass vial and the NIR probe was immersed into the sample. The Raman signal was measured through a quartz window. Data was gathered every 15 min. Each NIR experiment was carried out in triplicate and Raman experiments in duplicate.

Physical characterization of materials

Near infrared spectroscopy (NIR)

NIR spectra of all the binary mixtures and raw materials were determined using a 256 InGaAs diode array detector and a tungsten light source (Control Development Inc., South Bend, IN). Spectra of the wavelength interval of 1100–2200 nm were gathered. An average spectrum of 32 scans was obtained. The lactose samples were measured with two different setups: with a lamp, which had an effective sampling area of 10–20 mm (integration time was 0.025 s) and with an immersion probe, which had an effective sampling area of 1–2 mm (integration time was 0.035 s). To increase the sampling area for the probe setup, a rotating sample holder was used. The trehalose samples were measured using only the probe setup.

Raman spectroscopy

A Raman spectrometer (Control Development Inc., South Bend, IN) with a diode laser (excitation wavelength 785 nm)

(Starbright 785 S; Torsana Laser Technologies, Skodsborg, Denmark) was used to measure the spectra of the binary mixtures and raw materials. The spectra were gathered over 300–1500 cm^{-1} using a rotating sample holder. The integration time was 2 s and three scans were averaged. For each sample the spectra were recorded in triplicate.

X-ray powder diffraction (XRPD)

X-ray powder diffractometry was used to characterize the spray-dried and crystalline materials and the binary mixtures. The XRPD analysis was performed using a θ-θ diffractometer (Bruker AXS D8 Advance; Bruker AXS GmbH, Karlsruhe, Germany). The measurements were performed in symmetrical reflection mode with CuK_α radiation (1.54 Å) at 40 mA and 40 kV using Göbel mirror bent gradient multilayer optics. The scattered intensities were measured with a scintillation counter. The measurements were performed at 2θ range 10–25° for lactose samples and 10–35° for trehalose samples with a step size of 0.05° and a measuring time of 1 s/step. A rotating sample holder was used to decrease the effect of preferred orientation on the diffraction pattern. The experimental diffraction patterns were compared with the theoretical ones, which were based on the data obtained from the Cambridge Crystallographic Data Centre (CCDC) with Cerius2 (Diffraction-Crystal module; Accelrys Inc., Cambridge, UK). The data from the ref codes LACTOS10, BLACTO02 and TREHAL10 were used to generate the theoretical diffraction patterns of α-lactose monohydrate, β-lactose anhydrate and trehalose dihydrate, respectively (Fries et al 1971; Brown et al 1972; Garnier et al 2002).

The crystallinities of the samples were estimated by fitting the intensities of the crystalline and amorphous component to the experimental XRPD intensity curve. The intensity curve from totally amorphous sample (100%) was used as the amorphous model intensity curve. The crystalline model intensity curves consisted only of the diffraction reflections of the samples. The crystallinities were calculated as the ratio of the integrals of the intensities of the crystalline component and the studied sample. The accuracy of these analyses is ± 10%.

Development of the quantitation model

Partial least squares (PLS) regression was applied to obtain quantitative information about the NIR and Raman spectra (Simca-P v.10.5; Umetrics AB, Umeå, Sweden). The data was randomly divided into two sets to create (2/3 of samples) and to test (1/3 of samples) the model. Spectral variation, unrelated to sample composition, is always present. This results from instrumental noise, slight sampling geometry differences and sample effects such as particle size differences. Quantitative analysis is often improved if this variation is removed using spectral pre-processing. Several different pre-processing and scaling techniques were applied. The techniques for pre-processing the spectra were standard normal variate transformation (SNV) (Barnes et al 1989), multiplicative scatter correction (MSC) (Geladi et al 1985) and 1st and 2nd differentiation. SNV transformation is defined as:

$$x_{ik,SNV} = (x_{ik} - \bar{x}_i) \Big/ \sqrt{\frac{\sum (x_{ik} - \bar{x}_i)^2}{(K-1)}} \quad (1)$$

where $k = (1, \ldots . K)$ is the wavelength and i is the spectrum $\bar{x}_i = \Sigma i x_i / K$. In MSC correction, each spectrum x_i is normalized by regressing it against the average spectrum, ($m_k = \Sigma x_{ik} / n$), using:

$$x_{ik} = a_i + b_i m_k + e_{ik} \quad (2)$$

This gives the MSC corrected spectrum:

$$x_{ik,corrected} = (x_{ik} - a_i) / b_i \quad (3)$$

Unit variance and centering (UV) or just centering (Ctr) were used for scaling the variables. In unit variance scaling, the intensity at each measured wavelength or wavenumber is scaled to unit variance about the mean intensity. In centering the variables are centered by subtracting their averages. Different spectral regions were also tested. The goodness of the model was evaluated based on the root mean square errors of calibration and prediction (RMSEC and RMSEP, respectively).

Results and Discussion

Physical state of the sugars

The crystalline α-lactose monohydrate and trehalose dihydrate corresponded with the theoretical diffraction patterns that were based on the ref codes LACTOS10 and TREHAL10, respectively (Figure 1). Based on the XRPD patterns, both of the sugars were amorphous after spray drying, since a halo pattern without any distinct diffraction reflections was observed. In this study, amorphous lactose crystallized as a mixture of α-lactose monohydrate and β-lactose anhydrate. The appearance of β-lactose anhydrate in the sample could be verified by the appearance of the typical diffractions of β-lactose anhydrate (ref code BLACTO) in the XRPD pattern.

NIR spectroscopy detects the overtones and combinations of the non-harmonic vibrations that are seen in the IR region, such as stretching and bending. Thus, hydrogen bonds (OH, NH, CH and SH) are active in NIR spectroscopy. Amorphous and crystalline sugars can be differentiated based on their NIR spectra (Figure 2). When comparing the amorphous state to the crystalline hydrate, the most significant changes in the spectra can be seen in the 1900–1980 nm and 1400–1460 nm regions, where the bands caused by OH stretch and OH deformation of water molecules appear. When water is as a hydrate, the molecules are organized in the crystal lattice, thus, the band caused by hydrate water is narrower than when the water molecules are randomly organized in an amorphous matrix.

In the Raman spectra of the two amorphous carbohydrates, it can be noted that all of the bands are broader and begin to merge together (Figure 3). The amorphous spectra, thus, resemble spectra of the sugars in aqueous solution in a way that there is no long-range order (Söderholm et al 1999). However, there may be some differences due to short-range order. Like in a solution, the molecules in the amorphous

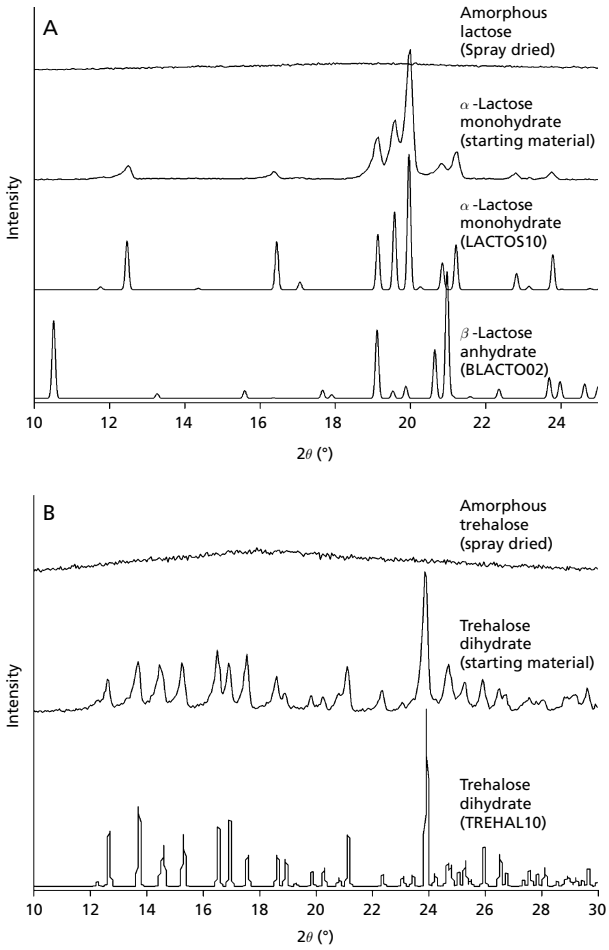

Figure 1 XRPD patterns of amorphous lactose, α-lactose monohydrate and theoretical diffraction patterns of α-lactose monohydrate (ref code LACTOS10) and β-lactose anhydrate (ref code BLACTO02) (A) and amorphous trehalose, trehalose dihydrate and theoretical diffraction pattern of trehalose dihydrate (ref code TREHAL10) (B).

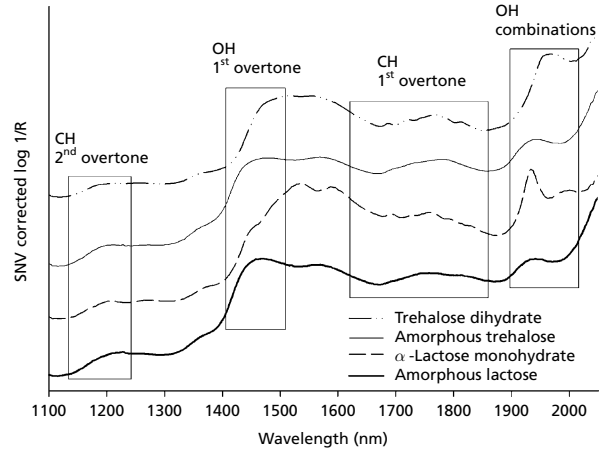

Figure 2 NIR spectra of lactose and trehalose in amorphous and crystalline states.

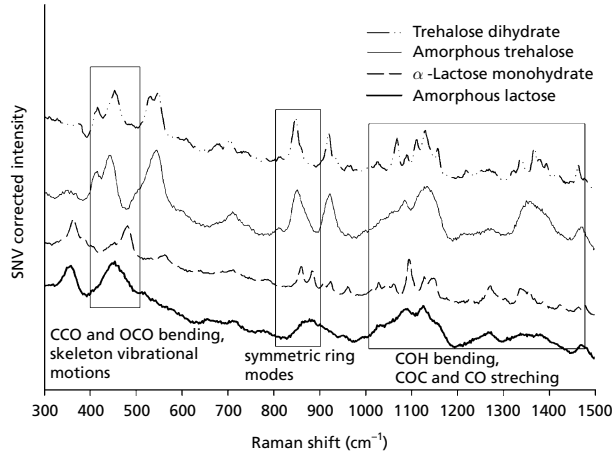

Figure 3 Raman spectra of lactose and trehalose in amorphous and crystalline states.

state exist in random conformations. These random conformations, as well as random packing, lead to band merging. For disaccharides, intensive peaks are observed in two regions 300–600 cm^{-1} and 800–1500 cm^{-1}. In the low wavenumber region, skeleton vibrational motions (325–490 cm^{-1}) as well as COC bending (~350 cm^{-1}) and CCO and OCO bending (400–500 cm^{-1}) are observed (Susi & Ard 1974; Kačuráková & Mathlouthi 1996; Nørgaard et al 2005). In the higher wave number region, symmetric ring-modes in the anomeric region (820–900 cm^{-1}), COC stretching vibrations (1000–1100 cm^{-1}), as well as CO stretching and COH bending motions (900–1500 cm^{-1}) are noted. A significant peak shift from 480 cm^{-1} to 453 cm^{-1} is observed, when comparing lactose in the crystalline and amorphous states. In the trehalose spectra, this peak shift is smaller, from 453 cm^{-1} to 444 cm^{-1}.

Development of the quantitation models

NIR model

A spectral region of 1100–2050 nm was chosen for quantitation, since at higher wavelengths the background noise causes disturbance in the spectra during the real-time process measurements. Various physical sample properties, such as particle size or differences in path lengths, cause offsets on the base line of the spectra. Thus, pre-processing and the scaling of the spectral data improve all of the models significantly.

The SNV correction was the best pre-processing method. When the lamp setup was used for the analysis of the lactose samples and when the whole spectral region was used, scaling of the data to unit variance (UV) improved the model (RMSEC = 2.4% and RMSEP = 2.7%) (Table 1). All the samples were stored at 0% r.h. but the amorphous particles absorbed some moisture during the measurements, which can be detected by the small band at the 1900–1980 nm region in the 100% amorphous sample. Based on the weights plot, the change from absorbed free water of the amorphous sugars to hydrate water at the 1920–1980 nm and 1400–1460 nm regions seemed to have a significant effect on the multivariate

Table 1 Assessment of different preprocessing and scaling methods for NIR spectra of lactose (lamp setup)

Amorphous content	Pre-process. method	Wavelength (nm)	Scaling	PLS factors	R2Y	Q2Y	RMSEC (%)	RMSEP (%)
0–100%	Raw data	1100–2050	None	2	0.99	0.99	6.0	5.4
			UV	3	0.99	0.99	4.1	5.0
			Ctr	3	0.99	0.99	3.3	4.1
0–100%	1st derivative (25 points)	1100–2050	None	2	1.00	1.00	3.6	4.1
			UV	2	0.99	0.99	3.0	3.8
			Ctr	2	0.99	0.99	3.0	3.7
0–100%	2nd derivative (45 points)	1100–2050	None	2	1.00	1.00	4.1	4.6
			UV	2	0.99	0.99	4.1	4.3
			Ctr	2	0.99	0.99	2.9	3.5
0–100%	MSC	1100–2050	None	2	1.00	1.00	3.9	3.6
			UV	1	0.99	0.99	3.8	3.7
			Ctr	1	0.99	0.99	3.9	3.6
0–100%	SNV	1100–2050	None	2	1.00	1.00	3.4	3.1
			UV	2	1.00	1.00	2.4	2.7
			Ctr	1	0.99	0.99	3.7	3.4
		1100–1599	None	2	1.00	1.00	2.4	2.5
			UV	1	0.99	0.99	3.4	3.7
			Ctr	1	1.00	1.00	2.6	2.6
		1600–1799	None	2	0.98	0.98	7.9	7.6
			UV	2	0.98	0.98	4.6	4.5
			Ctr	2	0.99	0.99	3.9	3.6
		1800–2050	None	2	1.00	1.00	2.8	2.5
			UV	2	0.99	0.99	3.1	2.9
			Ctr	1	0.99	0.99	3.5	3.2
0–10%	SNV	1100–2050	UV	4	0.99	0.98	0.4	0.6
10–90%		1100–2050	UV	1	0.99	0.99	2.6	3.1
90–100%		1100–2050	UV	2	0.92	0.91	1.0	1.4

R2Y, correlation coefficient; Q2Y, cross-validation coefficient; RMSEC/P; root mean square error of calibration/prediction.

model (Figure 4). The water–solid interactions are different in the crystalline and amorphous states. Unlike in the amorphous sugars, in the sugar hydrates the molecules are well organized in the crystal lattice and, thus, the bands are narrower.

The measuring setup and effective sampling area also influenced the model. The effective sampling area is known to affect the quality of the model (Johansson et al 2005; Wikström et al 2005). Increasing the sampling area can improve the model. Therefore, the quantitation model for lactose was more accurate when the lamp setup was used rather than the probe, due to the larger sampling area (Figure 5). However, the variability of the predicted concentration increases at the low and high levels of amorphous content. For more precise analysis at close to 100% of either form, separate models at either end of the composition range should be created. The best quantitation model for the probe setup (SNV corrected and UV scaled data) was obtained when the spectral region of 1100–2050 nm was used. The RMSEC and RMSEP were 3.9% and 4.3%, respectively. As with lactose, the best quantitation model for trehalose was obtained when a wide spectral region (1100–2050 nm) was used (SNV corrected and Ctr scaled data), with the RMSEC and RMSEP both 4.2%.

Depending on the experimental conditions (e.g. relative humidity) under which the change in amorphousness is monitored, it is often useful to build the quantitation model on a smaller spectral region. If NIR spectroscopy is used to detect changes in the amorphous content in an environment where water is present, it can be useful to build the model on a spectral region where water is not detected, such as the 1600–1800 nm region. The advantage in using this region is that the bands caused by OH stretch and OH deformations of water molecules (1900–1980 nm and 1400–1460 nm) do not affect the model.

The SNV is more suitable than the MSC for process analytical purposes, where spectra are gathered continuously, since the MSC needs to refer to other spectra, whereas in SNV the spectra are treated individually (Barnes et al 1989; Geladi et al 1985). Therefore, the PLS model based on SNV correction using the whole spectral region was chosen as the regression model for the amorphization of crystalline material. In addition 1st and 2nd derivatives of the absorbance spectra may cause problems in the process environment, since they tend to emphasize background noise.

Often small amounts of amorphous material or small degrees of crystallinity are created unintentionally during processing or storage. When the aim is to detect small changes in amorphousness or crystallinity, it is best to build the quantitation model for a smaller composition range. For example, the quantitation model of lactose could be further improved by building three separate models: one for low amorphous contents (0–10%), one for 10–90% amorphousness and one for high amorphous contents (90–100%) (Table 1).

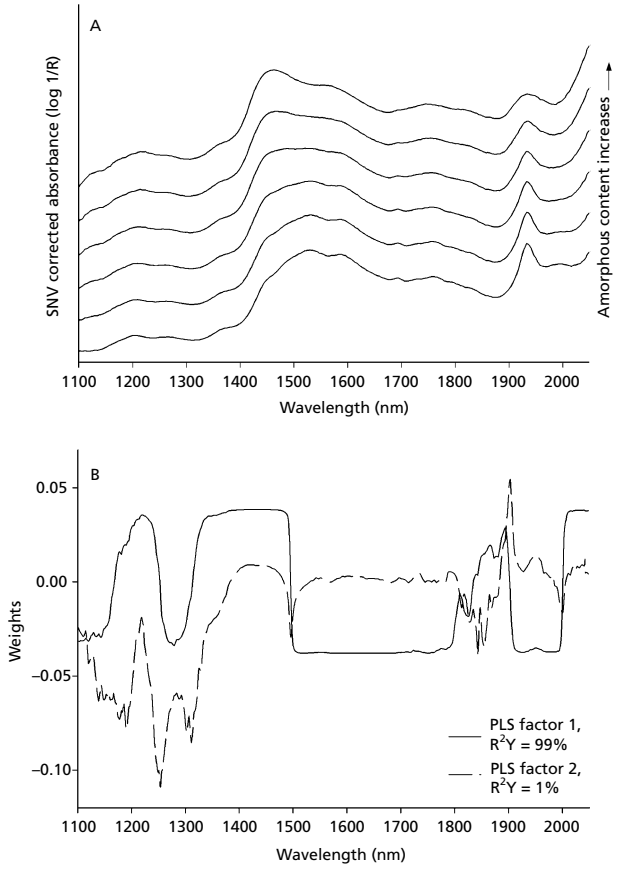

Figure 4 SNV corrected spectra of the different lactose compositions (0–100% w/w) analysed by NIR spectroscopy (A) and PLS weights plot (B).

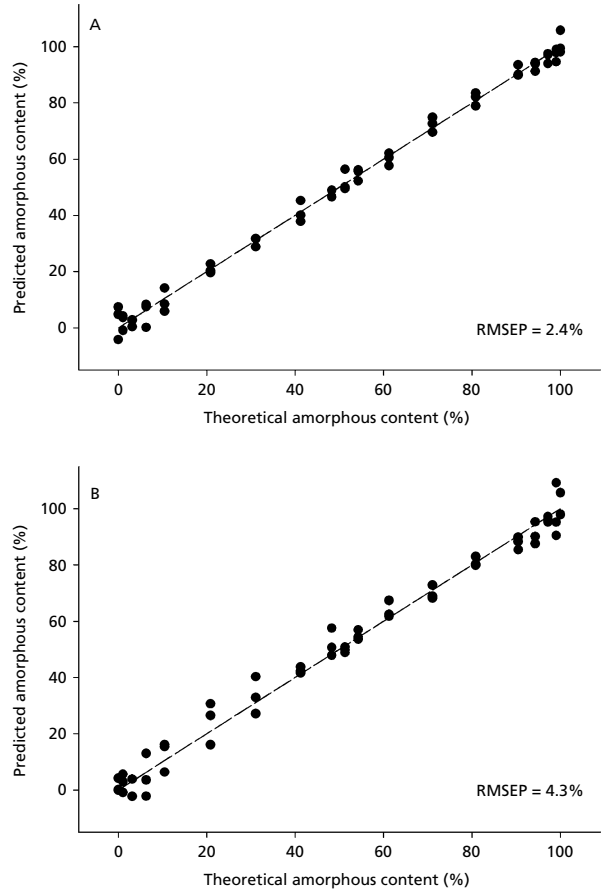

Figure 5 Theoretical versus predicted amorphous content of lactose after analysis with NIR. A. Lamp setup (1100–2050 nm, SNV corrected, UV scaled). B. Probe setup (1100–2050 nm, SNV corrected and UV scaled).

Raman model

The spectral region of 300–1500 cm^{-1} was chosen since no distinct peaks were noted after 1500 cm^{-1}. Similarly as for the NIR spectroscopic data, pre-treatment of the data was necessary. The PLS model created for the quantitation of lactose, using the SNV correction as a pre-treatment method and centering (Ctr) as a scaling method, had the smallest RMSEC and RMSEP values of 2.4% and 2.3%, respectively (Table 2). Due to merging of the peaks and overlapping peaks in the amorphous state, the usage of a wider spectral region (300–1500 cm^{-1}) seemed to be the best data selection technique. Three PLS factors were needed (Figure 6). The merging of the peaks in the 1010 cm^{-1} to 1180 cm^{-1} region, as well as, the peak shift from 453 cm^{-1} to 480 cm^{-1} seemed to have a significant influence on the multivariate model. For trehalose, the best quantitation model was obtained also using the 300–1500 cm^{-1} region (SNV corrected and Ctr scaled data, RMSEC = 2.2% and RMSEP = 2.5%).

If the aim is to determine small changes in the amorphous content, such as small amounts of crystalline material in amorphous matrix or vice versa, a more accurate quantitation model is obtained if separate models are built for the far ends of the composition ranges (Table 2).

Quantitation of amorphous content in process environment

Amorphization of crystalline material

Amorphization of crystalline model substance, α-lactose monohydrate, was performed by grinding the sample in a ball mill. The increase in the amorphous content could be monitored on-line with both Raman and NIR spectroscopy. Process data differs often from the calibration data (e.g. there is more background noise). Even though the best model for quantitation using Raman spectroscopy was the SNV corrected and Ctr scaled model, the model did not work in the process environment due to intensity differences in the process and calibration data. Intensity differences were probably caused by tighter packing of the particles and reflections caused by the metal milling bowl. Therefore, the model was based on the spectral region, where the process data resembled the calibration data most (1000–1500 cm^{-1} region). The spectra were SNV corrected and UV scaled (RMSEC = 3.2% and RMSEP = 3.4%).

The milling process induced a change from α-lactose monohydrate to amorphous lactose. Thus, the hydrate water

Table 2 Assessment of different preprocessing and scaling methods for Raman spectra of lactose

Amorphous content	Pre-process. method	Wavenumber (cm^{-1})	Scaling	PLS factors	R2Y	Q2Y	RMSEC (%)	RMSEP (%)
0–100%	Raw data	300–1500	None	2	0.99	0.99	6.0	6.5
			UV	3	0.99	0.99	4.3	4.6
			Ctr	2	0.98	0.98	5.2	5.5
0–100%	1st derivative (25 points)	300–1500	None	2	0.99	0.99	5.2	5.6
			UV	1	0.98	0.98	4.8	4.8
			Ctr	1	0.98	0.98	5.3	5.6
0–100%	2nd derivative (35 points)	300–1500	None	2	0.99	0.99	5.4	5.7
			UV	2	0.98	0.98	4.6	4.8
			Ctr	2	0.98	0.98	4.6	5.0
0–100%	MSC	300–1500	None	2	0.98	0.98	8.4	8.7
			UV	2	0.96	0.99	7.5	8.1
			Ctr	3	0.98	0.96	5.2	7.5
0–100%	SNV	300–1500	None	2	0.99	0.99	7.9	8.1
			UV	3	0.99	0.99	3.0	3.0
			Ctr	3	1.00	0.99	2.4	2.3
		300–600	None	2	1.00	1.00	4.3	4.8
			UV	2	0.99	0.99	3.5	3.9
			Ctr	2	0.99	0.99	2.8	2.8
		600–1000	None	2	0.98	0.98	9.3	9.4
			UV	3	0.99	0.98	3.6	4.6
			Ctr	3	0.99	0.99	3.4	4.3
		1000–1500	None	2	0.99	0.99	4.8	4.8
			UV	2	0.99	0.99	3.2	3.4
			Ctr	2	0.99	0.99	2.8	3.0
0–10%	SNV	300–1500	Ctr	4	0.99	0.83	0.3	1.9
10–90%			Ctr	3	1.00	0.99	1.4	2.7
90–100%			Ctr	3	0.99	0.96	0.2	0.8

R2Y, correlation coefficient; Q2Y, cross-validation coefficient; RMSEC/P, root mean square error of calibration/prediction.

of the α-lactose monohydrate was released and resorbed into the amorphous regions. This water had to be taken into consideration when building the quantitation model for NIR spectroscopy, since the samples used for the calibration set were stored at 0% r.h. and did not have sorbed moisture in them (Figure 7A). Therefore, the 1900–2000 nm region, where water is detected, was left out of the quantitation model (SNV corrected and UV scaled spectra, RMSEC = 2.5%, RMSEP = 2.8%). However, the 1400–1460 nm region was included in the model, even though water is also detected in this region. The changes in the spectra in this region were not as significant and the removal of this region did not improve the model.

When the quantitation was based on NIR or Raman data, the amorphous contents detected were similar to the XRPD results (Figure 7B). However, the standard deviation is larger when measuring with Raman. The differences between NIR and Raman results are probably due to the differences in the measuring techniques and effective sampling areas. The amorphous content of the ground material varies at different locations in the grinding bowl. The area where spectral information is gathered is much smaller in the Raman spectroscopy (100–200 μm) than in the NIR spectroscopy (10–20 mm, lamp setup) and this causes more deviation in the replicate spectra. The XRPD patterns, on the other hand, were measured off-line and they represent average crystallinity at each time point, since the samples were gathered from a larger area all around the grinding bowl. Spectroscopic techniques not only provide a tool to monitor the changes in the amorphous content during milling, but they can also be used as a fast and easy method to monitor amorphousness at different locations of the bowl. However, the variation could also be used to describe the state of the process and to determine the end-point of milling.

Crystallization of amorphous material

The storage of amorphous lactose and trehalose at 85% r.h. at room temperature could be used to represent the crystallization of amorphous substances. An in-line measuring setup was possible for both of the spectroscopic techniques. These techniques combined with chemometrics could be used to monitor the crystallization kinetics. Quantitation of amorphous content was possible only for the trehalose samples. The Raman spectra of the process data and calibration data differed and significant intensity differences occurred at higher wavenumbers. Therefore, the model was built on the lower wavenumber region (300–1000 cm^{-1}) using SNV corrected and UV scaled data (RMSEC = 2.1%, RMSEP = 2.6%) (Figure 8). The XRPD analysis verified the amorphous content at the end of the experiment. The estimated amorphous content at the end of the experiment based on XRPD data was 20% (±10%).

In addition to the change in amorphousness, the processing and the environmental conditions can affect the spectra.

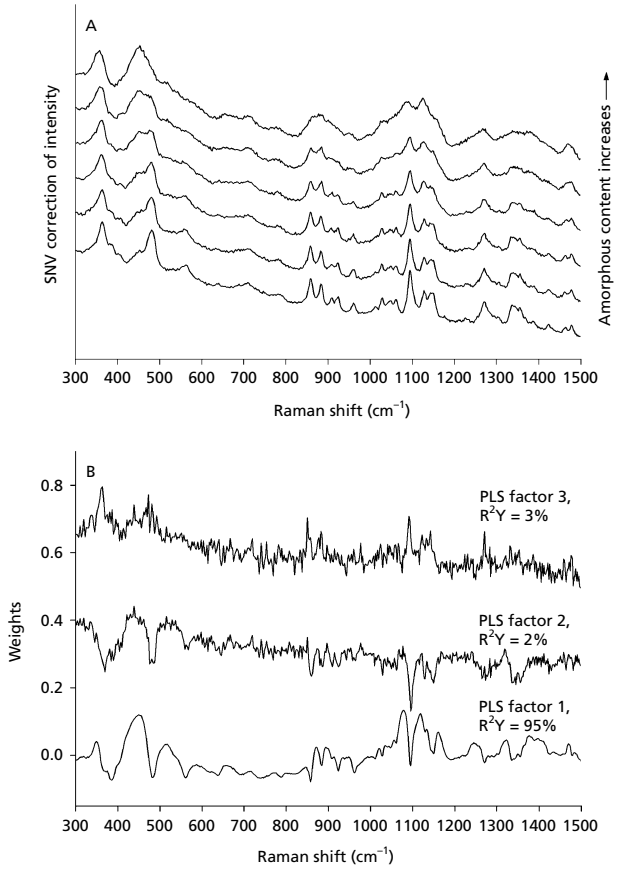

Figure 6 SNV corrected spectra of the different lactose compositions (0–100% w/w) analysed by Raman spectroscopy (A) and PLS weights plot (B). The PLS weights plots presented with an increasing offset of 0.3.

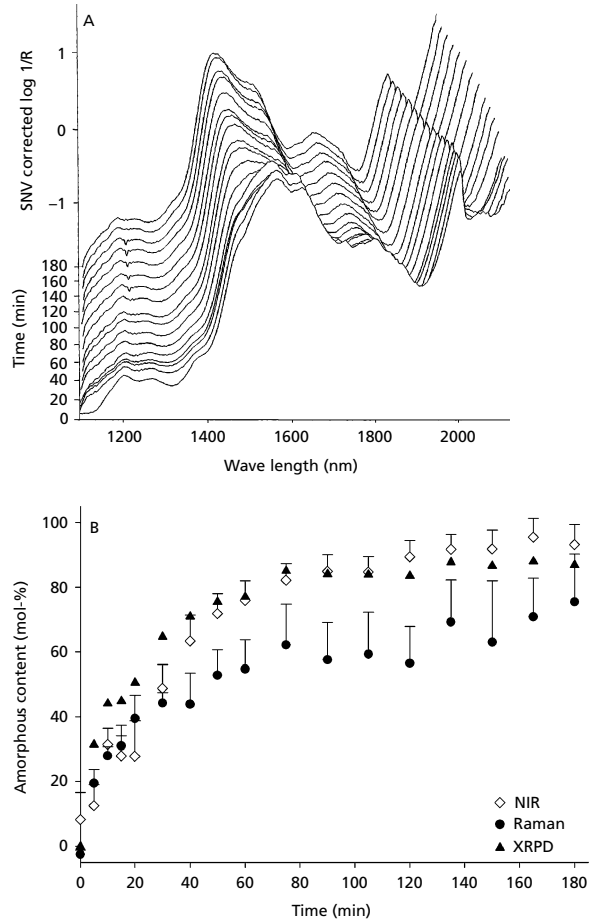

Figure 7 A. NIR spectra of lactose obtained during milling. B. The amorphous content of lactose during milling determined by NIR, Raman and XRPD analysis.

In an ideal situation the data for the quantitation model should be constructed in the same environment in which the process analysis is performed. When amorphous material is stored at high relative humidity, it sorbs moisture due to its hygroscopicity. Since NIR is sensitive to water, this sorption of water has to be taken into consideration when selecting the PLS model. The quantitation model was, therefore, built based on the regions where water is not detected (1100–1400 nm, 1500–1900 nm, 2000–2050 nm) (SNV corrected and Ctr scaled data, RMSEC = 6.4%, RMSEP = 6.4%) (Figure 9). However, these regions were also those where the spectral differences between the amorphous and crystalline samples were less distinct and, therefore, the NIR model was not as good as the Raman one. The estimated amorphous content at the end of the experiment based on XRPD data was 20% (± 10%).

The multivariate model could not be used to quantify the amount of amorphous lactose in the samples, since amorphous lactose crystallized as a mixture of α-lactose monohydrate and β-lactose anhydrate, which can be verified by the appearance of the typical peaks of α-lactose monohydrate and β-lactose anhydrate in the XRPD pattern at 16.4° 2θ and 10.5° 2θ, respectively (Figure 10A). In previous studies, lactose stored at relative humidity higher than 50% crystallized as various polymorphs and mixtures of polymorphs, where the most common forms were α-lactose monohydrate, anhydrous β-lactose and a mixture of anhydrous crystals with α-lactose and β-lactose in molar ratio of 5:3 or 4:1 (Briggner et al 1994; Buckton & Darcy 1996; Jouppila et al 1998; Haque & Roos 2005). This was not taken into consideration when building up the model and, therefore, the appearance of β-lactose anhydrate in the samples led to failure of the quantitation. With trehalose this problem does not exist, since trehalose recrystallizes at 85% r.h. as only one polymorphic form, a dihydrate (Figure 10B). For the multivariate approach to work, all the forms present, such as various forms of lactose, have to be taken into consideration when building up the multivariate model.

When comparing the NIR and Raman data, a difference in the measured crystallization kinetics was noted. Both of the sugars crystallized during storage at high relative humidity, within 23 h when measuring with NIR spectroscopy, and within 11 h when measuring with Raman spectroscopy. The kinetics of crystallization vary depending on the experimental conditions, relative humidity and temperature (Roos & Karel 1992; Buckton & Darcy 1996; Jouppila et al 1998; Haque & Roos 2005). In this study, the differences in the kinetics were most likely caused by the differences in the experimental setups. The NIR studies were conducted in a bigger humidity chamber than the Raman measurements. The sample vials were also of different size and shape.

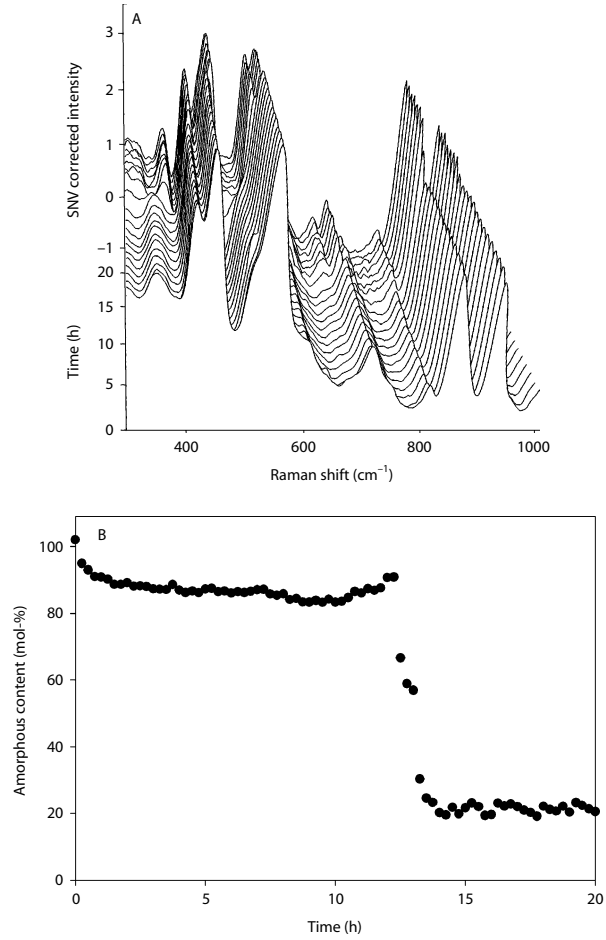

Figure 8 Determination of amorphous content of trehalose during storage at 85% r.h. using Raman spectroscopy; Raman spectra (A) and change in amorphous content (B).

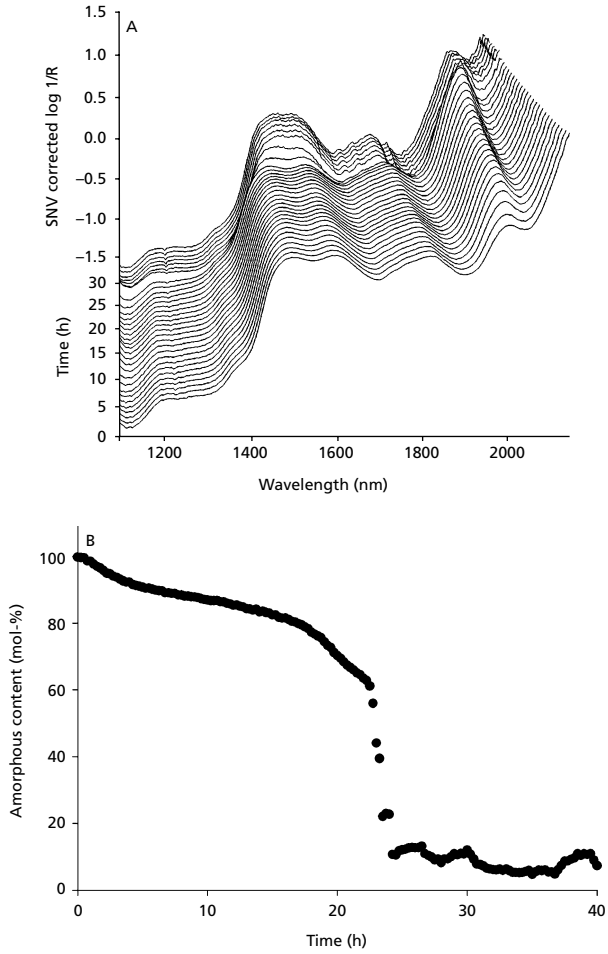

Figure 9 Determination of amorphous content of trehalose during storage at 85% r.h. using NIR spectroscopy; NIR spectra (A) and change in amorphous content (B).

Conclusions

Spectroscopic techniques (NIR and Raman) combined with a partial least squares (PLS) method could be used to follow process-induced transformations, which affect the amorphous content, during different unit operations. These spectroscopic approaches combined with multivariate techniques offer a non-destructive and fast method to monitor and quantify amorphous content of materials in a real-time mode. This will increase process understanding and, thus, increase the safety of medication.

References

Barnes, R. J., Dhanoa, M. S., Lister, S. J. (1989) Standard normal variate transformation and de-trending of near-infrared diffuse reflectance spectra. *Appl. Spectrosc*. **43**: 772–777

Briggner, L.-E., Buckton, G., Bystrom, K., Darcy, P. (1994) The use of isothermal microcalorimetry in the study of changes in crystallinity induced during the processing of powders. *Int. J. Pharm*. **105**: 125–135

Brown, G. M., Rohrer, D. C., Berking, B., Beevers, C. A., Gould, R. O., Simpson, R. (1972) The crystal structure of α,α-trehalose dihydrate from three independent X-ray determinations. *Acta Crystallogr*. **B28**: 3145–3158

Buckton, G., Darcy, P. (1996) Water mobility in amorphous lactose below and close to the glass transition temperature. *Int. J. Pharm*. **136**: 141–146

Buckton, G., Yonemochi, E., Hammond, J., Moffat, A. (1998) The use of near infra-red spectroscopy to detect changes in the form of amorphous and crystalline lactose. *Int. J. Pharm*. **168**: 234–241

FDA (2004) PAT — a framework for innovative pharmaceutical development, manufacturing, and quality assurance. In: *Guidance for industry*. U.S. Food and Drug Administration, Rockville, MD, page http://www.fda.gov/cder/guidance/6419fnl.pdf

Fries, D. C., Rao, S. T., Sundaralingam, M. (1971) Structural chemistry of carbohydrates. III. Crystal and molecular structure of 4-*O*-β-D-galactopyranosyl-α-D-glucopyranose monohydrate (α-lactose monohydrate). *Acta Crystallogr*. **B27**: 994–1005

Garnier, S., Petit, S., Coquerel, G. (2002) Dehydration mechanism and crystallisation behaviour of lactose. *J. Therm. Anal. Cal*. **68**: 489–502

Geladi, P., MacDougall, D., Martens, H. (1985) Linearization and scatter-correction for near-infrared reflectance spectra of meat. *Appl. Spectrosc*. **39**: 491–500

Gombás, Á., Antal, I., Szabó-Révész, P., Marton S., Erõsa I. (2004) Quantitative determination of crystallinity of alpha-lactose

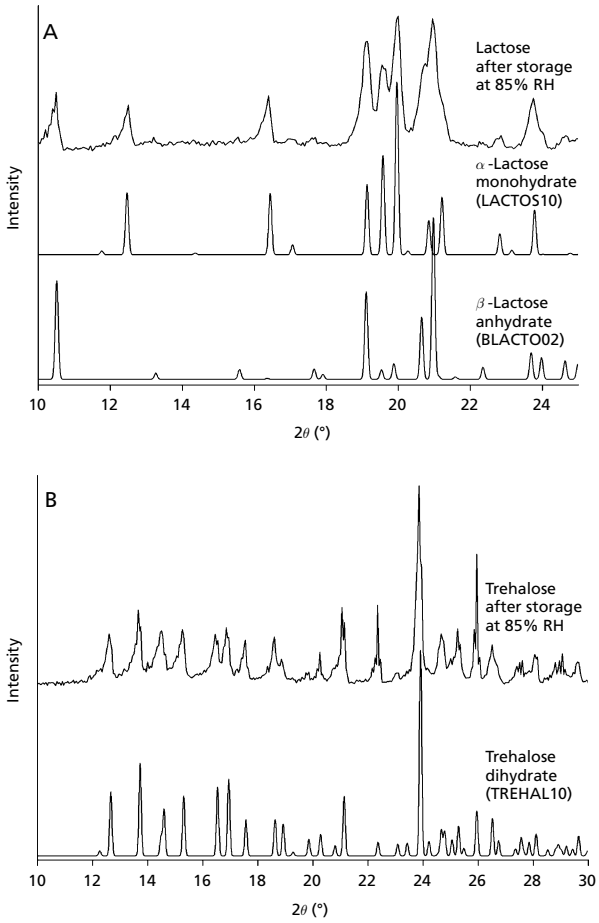

Figure 10 X-ray powder diffraction pattern of lactose (A) and trehalose (B) after crystallization from amorphous state. For comparison, theoretical diffraction patterns of α-lactose monohydrate (LACTOS10), β-lactose anhydrate (BLACTO02) and trehalose dihydrate (TREHAL10).

monohydrate by near infrared Spectroscopy (NIRS). *Int. J. Pharm*. **280**: 209–219

Grant, D. J. W. (1999). Theory and origin of polymorphism. In: Brittain, H. G. (ed.) *Polymorphism in pharmaceutical solids*. Vol. 95, Marcel Dekker, New York, pp 1–33

Haque, K. Roos, Y. H. (2005) Crystallization and X-ray diffraction of spray-dried and freeze-dried amorphous lactose. *Carbohydr. Res*. **340**: 293–301

Johansson, J., Pettersson, S., Folestad, S. (2005) Characterization of different laser irradiation methods for quantitative Raman tablet assessment. *J. Pharm. Biomed. Anal*. **39**: 510–516

Jouppila, K., Kansikas, J., Roos, Y. H. (1998) Crystallization and X-ray diffraction of crystals formed in water-plasticized amorphous lactose. *Biotechnol. Prog*. **14**: 346–350

Kačuráková, M., Mathlouthi, M. (1996) FTIR and laser-Raman spectra of oligosaccharides in water: characterization of the glycosidic bond. *Carbohydr. Res*. **284**: 145–157

Niemelä, P., Päällysaho, M., Harjunen, P., Koivisto, M., Lehto, V.-P., Suhonen, J., Järvinen, K. (2004) Quantitative analysis of amorphous content of lactose using CCD-Raman spectroscopy. *J. Pharm. Biomed. Anal*. **36**: 906–911

Nørgaard, L., Hahn, M. T., Knudsen, L. B., Farhat, I. A., Engelsen, S. B. (2005) Multivariate near-infrared and Raman spectroscopic quantifications of the crystallinity of lactose in whey permeate powder. *Int. Dairy J*. **15**: 1261–1270

Roos, Y. H., Karel, M. (1992) Crystallization of amorphous lactose. *J. Food Sci*. **56**: 665–666

Söderholm, S., Roos, Y. H, Meinander N., Hotokka M. (1999) Raman spectra of fructose and glucose in the amorphous and crystalline states. *J. Raman. Spectr*. **30**: 1009–1018

Susi, H., Ard, J. S. (1974) Laser-Raman spectra of lactose. *Carbohydr. Res*. **37**: 351–354

Taylor, L. S., Zografi, G. (1998) The quantitative analysis of crystallinity using FT-Raman spectroscopy. *Pharm. Res*. **15**: 755–761

Vippagunta, S. R., Brittain, H. G., Grant, D. J. W. (2001) Crystalline solids. *Adv. Drug Deliv. Rev*. **48**: 3–26

Wikström, H., Lewis, I. R., Taylor L. (2005) Comparison of sampling techniques for in-line monitoring using Raman spectroscopy. *Appl. Spectrosc*. **59**: 934–941